Proc. Natl. Acad. Sci. USA
Vol. 90, pp. 5006–5010, June 1993
Biochemistry

Differentiation and identification of the two catalytic metal binding sites in bovine lens leucine aminopeptidase by x-ray crystallography

(metal hybrid enzyme/catalytic mechanism/metalloenzyme)

HIDONG KIM AND WILLIAM N. LIPSCOMB*

Gibbs Chemical Laboratory, Harvard University, Cambridge, MA 02138

Contributed by William N. Lipscomb, February 18, 1993

ABSTRACT **The tightly binding and readily exchanging metal binding sites in the active site of bovine lens leucine aminopeptidase (blLAP; EC 3.4.11.1) have been differentiated and identified by x-ray crystallography. In native blLAP, Zn^{2+} occupies both binding sites. In solution, site 1 readily exchanges Zn^{2+} for other divalent cations, including Mg^{2+}. The Zn^{2+} in site 2 is unavailable for metal exchange under conditions which allow exchange at site 1. The Zn^{2+}/Mg^{2+} metal hybrid of blLAP (Mg-blLAP) was prepared in solution and crystallized. X-ray diffraction data to 2.9-Å resolution were collected at −150°C from single crystals of Mg-blLAP and native blLAP. Comparisons of omit maps calculated from the Mg-blLAP data with analogous maps calculated from the native blLAP data show electron density in one of the metal binding sites in Mg-blLAP which is much weaker than the electron density in the other binding site. Since there are fewer electrons associated with Mg^{2+} than with Zn^{2+}, the difference in electron density between the two metal binding sites is consistent with occupancy of the weaker electron density site by Mg^{2+} and identifies this metal binding site as site 1, defined as the readily exchanging site. The present identification of the metal binding sites reverses the previous presumptive assignment of the metal binding sites which was based on the structure of native blLAP [Burley, S. K., David, P. R., Sweet, R. M., Taylor, A. & Lipscomb, W. N. (1992) *J. Mol. Biol.* 224, 113–140]. According to the residue-numbering convention of native blLAP, the new assignment of the metal binding sites identifies the readily exchanging site 1 with Zn-488, which is within interaction distance of one side-chain carboxylate oxygen from each of Asp-255, Asp-332, and Glu-334 and the main-chain carbonyl oxygen of Asp-332. The more tightly binding site 2 is identified with Zn-489, which is within interaction distance of one side-chain carboxylate oxygen from each of Asp-255, Asp-273, and Glu-334 and the side-chain amine nitrogen of Lys-250.**

One of the most intriguing aspects of catalysis by bovine lens leucine aminopeptidase (blLAP), which cleaves the N-terminal residue from polypeptide substrates, is its dependence on two divalent metal cations. These metals occupy two distinct binding sites at the active site. In the native blLAP protomer, six of which comprise the hexameric holoenzyme, both metal binding sites are occupied by Zn^{2+}. These two sites differ greatly in their affinities for various divalent metal cations. Site 1, the readily exchanging site, exchanges Zn^{2+} for many other divalent cations, including Mg^{2+}, Mn^{2+}, and Co^{2+}, in solution. Site 2 binds Zn^{2+} much more strongly than does site 1, retaining its Zn^{2+} under conditions which allow exchange of the Zn^{2+} in site 1. The site 1 Zn^{2+} exchanges with other divalent cations in solution ~15 times faster than does the site 2 Zn^{2+} (1). Site 2 also appears to be more specific for Zn^{2+} than site 1 is. Although many different divalent cations bind in site 1, Co^{2+} is the only divalent cation other than Zn^{2+} which has been reported to bind stoichiometrically in site 2 (1, 2). Particularly relevant to the present study, Mg^{2+} is not bound in detectable amounts to inactive metal-free blLAP under conditions in which Zn^{2+} binds stoichiometrically to metal-free blLAP (metal cation concentration of 10 mM). Thus, it appears that Mg^{2+} binds only to site 1, and then only if site 2 is occupied by a divalent metal (1, 3). The nature of the metal binding sites in the closely related porcine kidney LAP (pkLAP) is very similar to that of blLAP (4). The hexameric holoenzyme of pkLAP also contains two metal binding sites per protomer (4–6). One of these sites readily exchanges its metal in solution, accommodating many divalent cations, including Zn^{2+}, Mn^{2+}, Mg^{2+}, Ni^{2+}, and Cu^{2+}. The other site binds its metal more tightly. Although Cd^{2+} appears to bind partially to this more tightly binding site, the Zn^{2+} content of this site in native pkLAP is unaffected by conditions which allow metal replacement at the readily exchanging site (4).

For both blLAP and pkLAP, each metal substitution at either site 1 or site 2 results in a change in the enzyme activity (1, 4). Further, for certain substrates, it appears that the catalytic functions of the two Zn^{2+}/Co^{2+} metal hybrids of blLAP are not the same. When L-leucineamide is the substrate, K_m and k_{cat} of the site 1 Co^{2+}/site 2 Zn^{2+} blLAP are 20 mM and 39 $\mu mol \cdot min^{-1} \cdot mg^{-1}$, whereas K_m and k_{cat} of the site 1 Zn^{2+}/site 2 Co^{2+} blLAP are 3.1 mM and 23 $\mu mol \cdot min^{-1} \cdot mg^{-1}$ (1). Earlier studies on the kinetics of blLAP and pkLAP indicated that k_{cat} was affected predominantly by site 1 metal substitution, and K_m predominantly by site 2 metal substitution (2, 4, 7). These conclusions were based on the hydrolyses of L-leucineamide and L-leucine anilides. Later studies on pkLAP-catalyzed hydrolyses of more physiologically relevant substrates having amino acid residues on both sides of the scissile bond indicated that both K_m and k_{cat} were significantly affected, though not to the same extent, by site 1 metal substitution (8). More recent studies of metal substitutions in blLAP have also concluded that changes in K_m and k_{cat} are not as clearly attributable to either site 1 or site 2 metal substitution as previously believed (1).

The recently reported x-ray crystal structures of native blLAP and its complex with the tight-binding inhibitor bestatin have revealed the two metal binding sites (9–11). However, electron density maps did not indicate which metal is more weakly or strongly bound. A presumptive assignment of the site 1 and site 2 metal binding sites was made based on the protein ligand environment of each of the Zn^{2+} ions in native blLAP (11). According to the residue-numbering con-

The publication costs of this article were defrayed in part by page charge payment. This article must therefore be hereby marked "*advertisement*" in accordance with 18 U.S.C. §1734 solely to indicate this fact.

Abbreviations: LAP, leucine aminopeptidase; blLAP bovine lens LAP; Mg-blLAP, Zn^{2+}/Mg^{2+} hybrid blLAP; pkLAP, porcine kidney LAP; MPD, 2-methyl-2,4-pentanediol; LV, L-leucyl-L-valine; LVTS, transition state of L-leucyl-L-valine.

*To whom reprint requests should be addressed.

vention of native blLAP, Zn-489 was assigned as the site 1 Zn^{2+} and Zn-488 was assigned as the site 2 Zn^{2+}.

Because of the critical importance of the active-site metals in catalysis, the further understanding of blLAP requires some knowledge of the functions of these two metals and, at least, a secure assignment of the two metal binding sites. We report here the differentiation and identification of the two metal binding sites in blLAP by x-ray crystallographic studies of the Zn^{2+}/Mg^{2+} metal hybrid blLAP (Mg-blLAP). The electron density maps of Mg-blLAP show that the electron density in one of the metal binding sites is much weaker than that of the other as compared with analogous maps of native blLAP, which show approximately equal electron density for both metal binding sites. Due to the difference in the number of electrons associated with Zn^{2+} and Mg^{2+}, the electron density seen in the metal binding sites of Mg-blLAP is consistent with occupation of the stronger electron density site by Zn^{2+} and the weaker electron density site by Mg^{2+}. Since it is known that only site 1, the readily exchanging metal binding site, accommodates Mg^{2+} (1, 3), the site with the weaker electron density as seen in the Mg-blLAP maps has been identified as site 1. From these electron density maps, it is clear that Zn-488 occupies site 1 and Zn-489 occupies site 2 in native blLAP. The results of this study reverse the previous presumptive assignment of the metal binding sites (11).

MATERIALS AND METHODS

Bovine calf eye lenses were purchased from Pel-Freez Biologicals, and received packed on wet ice, 1 day after slaughter. The isolated blLAP (1) was further purified by gel filtration chromatography. Typically, 2 ml of protein solution (10 mg/ml) in a storage buffer (50 mM Tris/50 μM $ZnSO_4$/200 mM NaCl, pH 7.8) was separated over a Sephadex G-100 column (55 cm × 2 cm) in the same buffer at a flow rate of 0.3 ml/min at 4°C. Fractions (1 ml) were monitored for protein by A_{280}. For native blLAP samples, those fractions containing the purified blLAP, as judged by SDS/15% PAGE, were pooled and concentrated to 6 mg/ml in storage buffer.

Mg-blLAP was prepared as reported (3). The fractions containing purified blLAP from the Sephadex G-100 column were pooled and dialyzed against 50 mM Tris/50 mM $MgSO_4$/200 mM NaCl, pH 9.0, at room temperature and then dialyzed against this same buffer at 38°C for 5 hr. Under these conditions, Mg^{2+} will replace the Zn^{2+} in metal binding site 1, but not the Zn^{2+} in site 2. The protein sample was finally dialyzed at room temperature against 50 mM Tris/50 μM $MgSO_4$/200 mM NaCl, pH 9.0, and then concentrated to 6 mg/ml. The exchange of Zn^{2+} with Mg^{2+} was verified by activity assays using L-leucineamide as substrate. Consistent with this metal exchange, the cleavage of L-leucineamide monitored at 238 nm at room temperature indicated much higher activity for the presumptive Mg-blLAP than for native blLAP (refs. 1 and 3; data not shown). The crystals used for data collection were grown from Mg-blLAP and native blLAP preparations which had specific activities of 200 and 27 $\mu mol \cdot min^{-1} \cdot mg^{-1}$, respectively.

All of the data were collected from a single Mg-blLAP crystal and a single native blLAP crystal. Crystals of Mg-blLAP and native blLAP were grown by vapor diffusion at room temperature. A hanging 20-μl drop of protein solution (6 mg/ml) was allowed to equilibrate against a 500-ml reservoir of a 1:1 (vol/vol) mixture of 2-methyl-2,4-pentanediol (MPD) and either 50 mM Tris/50 μM $MgSO_4$/pH 9.0, for Mg-blLAP, or 50 mM Tris/50 μM $ZnSO_4$/pH 7.8, for native blLAP (12). Hexagonal rodlike crystals appeared within 1 week. The Mg-blLAP crystals were at best 0.15 mm in diameter and 0.5 mm long. Although we have recently developed a macroseeding method (refs. 13 and 14; unpublished results) by which we can routinely obtain native blLAP crystals at least 0.35 mm in diameter and 1.0 mm long, this method was unsuccessful in increasing the size of the Mg-blLAP crystals. The native blLAP crystal from which x-ray diffraction data were collected was 0.2 mm in diameter and 0.6 mm in length. This crystal was grown without the aid of macroseeding.

X-ray diffraction data were collected at −150°C on a Siemens (Iselin, NJ) X-100A multiwire area detector. Graphite-monochromated Cu K_α radiation was produced by a Rigaku (Danvers, MA) RU-200 rotating-anode x-ray generator with a 300-μm focus cup operating at 50 kV and 80 mA. A Siemens LT-2 apparatus was used to maintain the temperature. For data collection, the crystals were mounted in a freestanding thin film of the MPD crystallization solution (15). Solutions with high MPD concentrations have been reported as good cryoprotective solvents (16). Since the crystallization and cryoprotective buffers were the same for these crystals, there was no danger of crystal damage due to osmotic shock in transferring the crystals from the hanging drops in which they grew, onto the cryoprotective freestanding thin film. The unit cell parameters of the Mg-blLAP crystal were $a = 129.1$ Å, $c = 120.2$ Å, and the cell parameters of the native blLAP crystal were $a = 129.8$ Å, $c = 120.7$ Å, as determined by the data collection software BUDDHA (17). The space group of both crystals was $P6_322$. For Mg-blLAP, 134,829 reflections between 30.0-Å and 2.9-Å resolution were recorded, of which 13,523 were unique (98% completeness). The merging R factor [$R_{merge} = \Sigma_{hkl}(\Sigma_i|I - \bar{I}|\Sigma_i I)$] for the Mg-blLAP data was 0.162. The 10,797 reflections between 10.0-Å and 2.9-Å resolution with intensity $> 2\sigma$ were used in the refinement of the Mg-blLAP structure. For native blLAP, 70,404 reflections between 30.0-Å and 2.9-Å resolution were recorded, of which 13,052 were unique (94% completeness). R_{merge} for the native blLAP data was 0.136. The 10,195 reflections between 10.0-Å and 2.9-Å resolution with intensity $> 2\sigma$ were used in the refinement of the native blLAP structure.

The structures of Mg-blLAP and native blLAP were determined by molecular replacement and refined by Powell minimization, using the apoenzyme (metal-free enzyme) portion of the blLAP-amastatin complex (unpublished results) as the starting model. This model was chosen instead of the previously reported structure of native blLAP (11) because the blLAP–amastatin structure was refined against data collected at −150°C whereas the previously reported native blLAP structure was refined against data collected at room temperature. After Powell minimization refinement of the apoenzyme portions of Mg-blLAP and native blLAP, $F_o - F_c$ electron density maps clearly showed the difference in electron density in the metal binding sites between the two structures. In the Mg-blLAP maps, the electron density associated with one of the metal binding sites was much weaker than that of the other, whereas in analogous native blLAP maps, the electron densities associated with both metal binding sites appeared approximately equal. Zn^{2+} was built into the stronger electron density site and Mg^{2+} was built into the weaker electron density site of Mg-blLAP, and the entire structure was subjected to further Powell minimization refinement and B-factor refinement to a final crystallographic residual [$R_{factor} = \Sigma_{hkl}(||F_o| - |F_c||/F_o)$] of 0.189. The rms deviations from ideality for bond lengths and bond angles are 0.016 Å and 3.6°. The average B factor for the Mg-blLAP structure is 12 Å^2. Likewise, Zn^{2+} was built into both metal binding sites of native blLAP, and further Powell minimization and B-factor refinement resulted in an R_{factor} of 0.188. The rms deviations from ideality for bond lengths and bond angles are 0.016 Å and 3.6°.The average B factor for the native blLAP structure is 10 Å^2. No waters were built into either structure. For both the Mg-blLAP and the native

blLAP structure, the amino acid chain of the enzyme consists of residues 1–11 and 15–484. Residues 12–14 and the three C-terminal residues 485–487 occur in solvent-exposed regions and have not been located in any of the x-ray crystal structures of blLAP (9–11). All crystallographic refinements were executed by X-PLOR (18, 19) on a (Digital) DECstation 3100. All model building was done on an Evans and Sutherland (Salt Lake City) PS390 graphics system interfaced with a (Digital) VAXstation 3200 using FRODO (20). In spite of the modest resolution of the data and the rather high R_{merge} values, the final R_{factor} values for both structures are reasonable, even without building in waters. Further, the stereochemical deviations are within acceptable limits, and the protein is clearly traceable from the density.

RESULTS AND DISCUSSION

Comparisons of $F_o - F_c$ maps calculated from the Mg-blLAP and native blLAP data for which the metals have been omitted from the structure-factor calculations clearly show a difference between the electron densities associated with the metal binding sites in the two structures (Fig. 1). In the native blLAP maps, the electron densities at both metal binding sites appear approximately equal. In the Mg-blLAP maps, the electron density at one of the metal binding sites is much weaker than that at the other site. This difference in electron density is undoubtedly due to the replacement of Zn^{2+}, with its 28 associated electrons, by Mg^{2+}, with its 10 associated electrons, in the weaker electron density site. Since Mg^{2+} replaces only the Zn^{2+} in site 1, the readily exchanging metal binding site (1, 3), the weaker electron density site has been clearly identified as site 1. The metal in this site is within interaction distance of one side-chain carboxylate oxygen from each of Asp-255, Asp-332, and Glu-334, and the backbone carbonyl oxygen of Asp-332. The other metal binding site, which shows persistently strong electron density in omit maps calculated from both Mg-blLAP and native blLAP data, has concomitantly been identified as site 2, the tightly binding site. The metal in this site is within interaction distance of one side-chain carboxylate oxygen from each of Asp-255, Asp-273, and Glu-334 and the side-chain amine nitrogen of Lys-250. According to the residue-numbering convention of native blLAP, the site identified as site 1 corresponds to Zn-488 and the site identified as site 2 corresponds to Zn-489 in native blLAP (Fig. 2; Table 1). This reverses the presumptive identification of the metal binding sites based on the structure of native blLAP in which Zn-488 was presumed to occupy site 2 and Zn-489, site 1 (11).

The *B*-factor refinement of the structure in which Zn^{2+} ions were built into both metal binding sites against the Mg-blLAP data provides further evidence for the replacement of Zn-488 in native blLAP with Mg^{2+} in Mg-blLAP. When Zn^{2+} was introduced in place of Mg-488 in the Mg-blLAP structure, the X-PLOR-refined *B* factor of Zn-488 was unacceptably high. For the structure of native blLAP refined against native blLAP data, the *B* factor for Zn-488 (site 1) is 9 Å^2 and that for Zn-489 (site 2) is 16 Å^2. For the structure of Mg-blLAP refined against Mg-blLAP data, the *B* factor for Mg-488 (site 1) is 5 Å^2 and that for Zn-489 (site 2) is 17 Å^2 (this assumes complete occupancy of site 2 by Mg^{2+}). For the di-Zn^{2+} structure refined against Mg-blLAP data, the *B* factor for Zn-488 (site 1) is 35 Å^2 and that for Zn-489 (site 2) is 13 Å^2. These results indicate that with respect to the Mg-blLAP data, Mg^{2+} is more appropriate than Zn^{2+} in position 488, which has been identified with metal binding site 1.

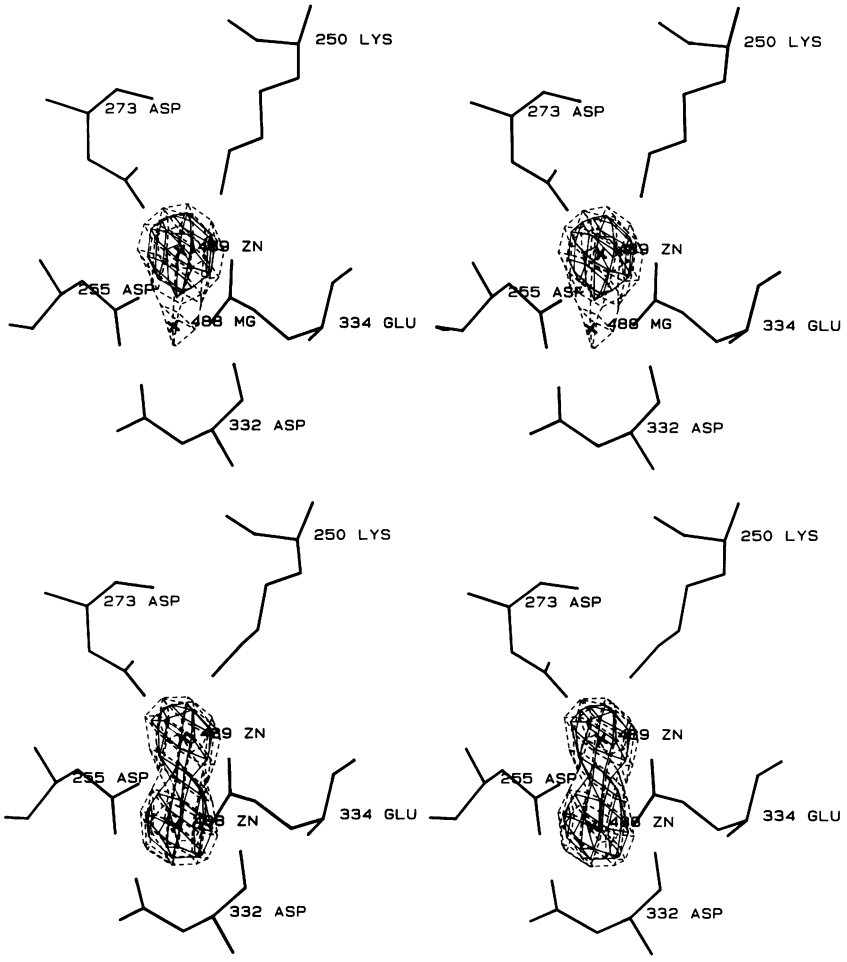

FIG. 1. (*Upper*) Stereoview of the active-site metal binding sites in Mg-blLAP. Shown is the electron density contoured at 7σ (broken lines) and 10σ (solid lines) of the $F_o - F_c$ map in which the metals were omitted from the structure-factor calculations. The refined coordinates of Lys-250, Asp-255, Asp-273, Asp-332, Glu-334, Mg-488, and Zn-489 are superimposed onto the map. (*Lower*) Stereoview of the active-site metal binding sites in native blLAP. Shown is the electron density contoured at 7σ (broken lines) and 9σ (solid lines) of the $F_o - F_c$ map in which the metals were omitted from the structure-factor calculations. The refined coordinates of Lys-250, Asp-255, Asp-273, Asp-332, Glu-334, Zn-488, and Zn-489 are superimposed onto the map.

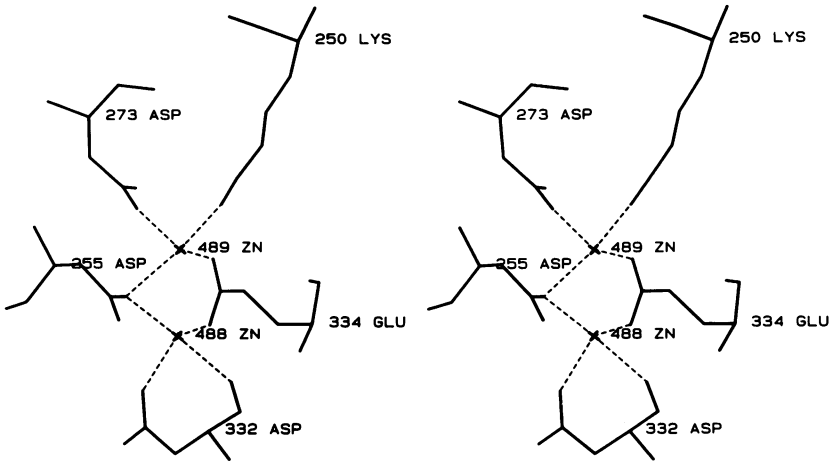

FIG. 2. Stereoview of the active-site Zn^{2+} coordination environment in native blLAP. The coordinates of Lys-250, Asp-255, Asp-273, Asp-332, Glu-334, Zn-488, and Zn-489 are taken from the 2.32-Å resolution structure of native blLAP (11). The amino acid–Zn^{2+} interactions listed in Table 1 are indicated by broken lines.

Even though the metals are within interaction distances of the amino acid atoms listed in Table 1, the geometries of all of these interactions are not optimal for metal coordination. The interactions of the metals with the side-chain carboxylate groups of Asp-255 and Asp-332 are not syn and in the plane of the carboxylates as Zn^{2+} ions are typically bound by carboxylates (21). Zn-488, the site 1 metal, is anti to the carboxylate of Asp-332 and 1.2 Å out of the plane of this carboxylate in the 2.32-Å structure of native blLAP (11). Zn-489, the site 2 metal, is anti to the carboxylate of Asp-255 and 2.0 Å out of the plane of this carboxylate in the 2.32-Å structure of native blLAP. The coordination of Zn-488 by the carboxylates of Asp-255 and Glu-334 and the coordination of Zn-489 by the carboxylates of Asp-273 and Glu-334 are syn and in the plane of the carboxylates. The unfavorable coordination geometries of Asp-332 to Zn-488 and of Asp-255 to Zn-489 most likely result in weaker binding for these interactions than for the other carboxylate–Zn^{2+} interactions.

The present identification of Zn-488 as the more weakly bound metal appears to be consistent with the protein ligand environment of the metals. One of the factors leading to the previous assignment of the metal binding sites was the ligation of Zn-489 by the side-chain amine nitrogen of Lys-250. It was believed that the tendency of the amine nitrogen to become protonated would disfavor its binding to the Zn^{2+}. Zn-488, which is coordinated by oxygens only, appeared to have the more stable ligands. However, if there is a weak ligand atom to one of the metals in these two sites, it is probably the backbone carbonyl oxygen of Asp-332, which coordinates to Zn-488 (or to Mg-488 in Mg-blLAP). The typical pK_a values of amine nitrogens, carboxylate oxygens, and carbonyl oxygens are 9–11, 4–5, and −4–0, respectively (22–26). The relative acidity of the carbonyl oxygen, combined with the poor binding geometry of the carboxylate, would most likely make Asp-332 a weak ligand of metal cations compared with the other residues listed in Table 1.

Table 1. Zinc coordination environment in native blLAP

Zinc	Ligand	Distance, Å
Zn-488 (site 1)	Asp-255 $O^{\delta 1}$	2.3 (2.2)
	Asp-332 backbone O	2.3 (2.4)
	Asp-332 $O^{\delta 2}$	2.1 (2.2)
	Glu-334 $O^{\epsilon 2}$	2.0 (2.2)
Zn-489 (site 2)	Lys-250 N^{ζ}	2.3 (2.3)
	Asp-255 $O^{\delta 1}$	2.6 (2.2)
	Asp-273 $O^{\delta 1}$	2.0 (2.2)
	Glu-334 $O^{\epsilon 1}$	2.1 (2.2)
	Zn-488	2.9 (2.9)

The first distance listed for each interaction is from the 2.32-Å resolution structure of native blLAP (11). The distances in parentheses are from the present structure of native blLAP.

Although it may be rather unusual to see a metal bound by a lysine side chain as Zn-489 is, the coordination of metal cations by alkylamines, such as ethylenediamine, in small-molecule complexes is not uncommon (27). Because the side-chain amine of Lys-250 is in the interior of the protein and near a Zn^{2+}, it is probably less susceptible to protonation than the side-chain amine of a lysine on the surface of the protein. At the basic pH values, 7.8 and 9.0, under which these experiments were done, the side-chain amine of Lys-250 in blLAP may exist to some extent in its unprotonated form, which would make it a plausible ligand for the metal.

Based on preliminary results on the refinement of the structure of the blLAP–amastatin complex (unpublished results), the dipeptide substrate L-leucyl-L-valine (LV) and its putative *gem*-diolate transition state (LVTS) were modeled into the active site of blLAP to determine plausible roles for the active-site metals in catalysis. It appears that in LAP catalysis, one of the metals, most likely the site 2 metal, is more important than the other. Although pkLAP, like blLAP, contains two metal binding sites, native pkLAP is active even though it contains only one bound metal. The lone metal, a Zn^{2+}, presumably occupies the tighter-binding metal site in pkLAP, which corresponds to site 2 in blLAP (4, 6). In the blLAP–LV model, there is a close interaction (2.1 Å) between the terminal amino nitrogen of LV and the site 2 Zn^{2+}. One aspect of the requirement of the site 2 metal in LAP catalysis appears to be the role of this metal in substrate binding via interactions with the terminal amino group of the substrate. A poor interaction between the substrate terminal amino and the site 2 metal may account for the observation that N-blocked species such as acetyl-L-tyrosineamide are not hydrolyzed by pkLAP whereas their corresponding species bearing a free N terminus are rapidly hydrolyzed (28). The scissile carbonyl oxygen of LV in the blLAP–LV model interacts with both active-site Zn^{2+} ions and also with the guanidinium nitrogens of Arg-336. By its interaction with the scissile carbonyl oxygen of LV, the site 1 metal may be involved in activating the substrate via an electrophilic polarization of the scissile carbonyl. Such a substrate carbonyl polarization would be enhanced by the guanidinium group of Arg-336. The presence of Arg-336 as an additional electrophile may obviate the requirement of the site 1 metal as in native pkLAP catalysis. The amino acid sequence of pkLAP is not known, so the presence of Arg-336 in pkLAP is not certain. However, Arg-336 is found in the *pepA*-encoded aminopeptidase from *Escherichia coli* and *Salmonella typhimurium* (29), so this residue may be conserved in other LAP as well.

The metals may also be involved in activating a water for nucleophilic attack on the scissile carbonyl of the substrate and in stabilizing the resulting *gem*-diolate transition state.

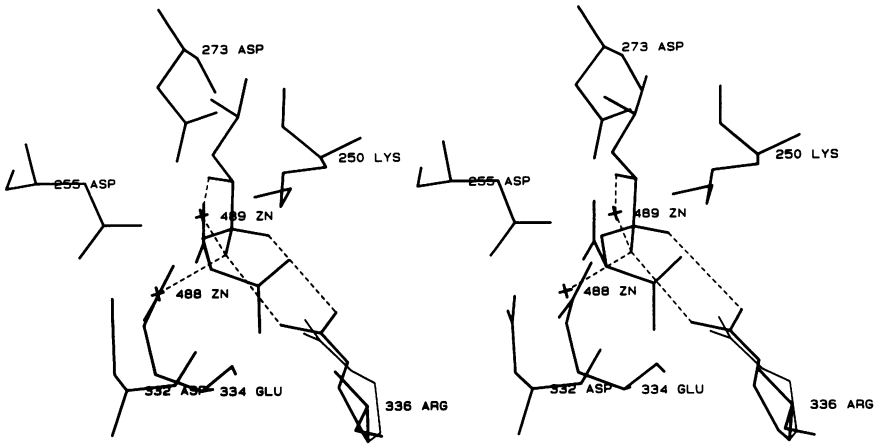

FIG. 3. Stereoview of the putative *gem*-diolate LVTS modeled into the active site of blLAP. The coordinates of Lys-250, Asp-255, Asp-273, Asp-332, Glu-334, Arg-336, Zn-488, Zn-489, and LVTS are shown. The *gem*-diolate oxygen O_a of LVTS is to the upper right of the *gem*-diolate oxygen O_b of LVTS in this view. O_a is assumed to be the former carbonyl oxygen of LV and O_b is assumed to be the water which attacks the scissile carbonyl carbon of LV from the left side of the active site in this view. O_b interacts with both Zn^{2+} ions and with $N_\eta 1$ of the guanidinium group of Arg-336. The interaction distance between the terminal amino nitrogen of LVTS and Zn-489 is 2.2 Å. The interaction distances between *gem*-diolate O_b of LVTS and Zn-488 and Zn-489 are 2.4 and 2.7 Å, respectively. The interaction distances between *gem*-diolate O_a of LVTS and $N_\eta 2$ of Arg-336 and between *gem*-diolate O_b of LVTS and $N_\eta 1$ of Arg-336 are 3.6 and 3.2 Å, respectively. These enzyme–ligand interactions are indicated by broken lines. The enzyme portion of this stereoview comes from preliminary refinement of the structure of the blLAP–amastatin complex (unpublished results). The conformation of the Arg-336 side chain in the blLAP–amastatin complex is shown in thin lines.

The current proposal for the mechanism of blLAP invokes a water to attack the scissile carbonyl of the substrate, leading to a *gem*-diolate transition state which is noncovalently bound to the enzyme (10). It is likely that such an attacking water is activated to a more nucleophilic hydroxide-like state via interactions with one or both of the metals. The pK_a values of metal-bound waters in proteolysis model systems have been measured to be as low as 7 (30). It is not clear whether one or both of the metals are involved in a possible water activation, since none of the x-ray crystallographic structural studies to date on blLAP indicates the presence of a metal-bound water (9–11). It may be that the site 2 metal is more important than the site 1 metal in water activation, since pkLAP is active even when only site 2 is occupied (4). Perhaps the binding of an active-site water to one or both of the metals in blLAP is too disordered to see at the 2.32-Å resolution limit of x-ray crystallographic studies on blLAP (11). Another possible explanation for the absence of a water in the x-ray crystal structures of blLAP is that the binding site for water develops as the substrate binds and is activated. The *gem*-diolate LVTS which would result from a water attack on LV was modeled into the active site of blLAP (Fig. 3). Both Zn^{2+} ions can participate in the stabilization of the tetrahedral intermediate via interactions with one of the *gem*-diolate oxygens. Further stabilization of LVTS can be provided by Arg-336. A modeled conformational change in the side chain of this residue allows it to participate in the stabilization of LVTS via a coplanar salt bridge between its positively charged guanidinium group and the negatively charged *gem*-diolate group of LVTS. The interactions of *gem*-diolate oxygen O_b (Fig. 3 legend) of LVTS with the active-site Zn^{2+} ions and Arg-336 may be a model for a water binding site which develops during catalysis.

A detailed proposal for the mechanism of blLAP catalysis, one featuring not only the metals but also important protein residues, must await further study. Additional aspects of LAP catalysis may be determined by further analyses of blLAP structures, such as the blLAP–amastatin complex which is currently under refinement.

We thank Prof. S. K. Burley for excellent discussions. This research was supported by National Institutes of Health Grant (GM06920) to W.N.L.

1. Allen, M. P., Yamada, A. H. & Carpenter, F. H. (1983) *Biochemistry* **22**, 3778–3783.
2. Thompson, G. A. & Carpenter, F. H. (1976) *J. Biol. Chem.* **251**, 1618–1624.
3. Carpenter, F. H. & Vahl, J. M. (1973) *J. Biol. Chem.* **248**, 294–304.
4. Van Wart, H. E. & Lin, S. H. (1981) *Biochemistry* **20**, 5682–5689.
5. Shen, C. & Melius, P. (1977) *Prep. Biochem.* **7**, 243–256.
6. Himmelhoch, S. R. (1969) *Arch. Biochem. Biophys.* **134**, 597–602.
7. Thompson, G. A. & Carpenter, F. H. (1976) *J. Biol. Chem.* **251**, 53–60.
8. Lin, W.-Y., Lin, S. H. & Van Wart, H. E. (1988) *Biochemistry* **27**, 5062–5068.
9. Burley, S. K., David, P. R., Taylor, A. & Lipscomb, W. N. (1990) *Proc. Natl. Acad. Sci. USA* **87**, 6878–6882.
10. Burley, S. K., David, P. R. & Lipscomb, W. N. (1991) *Proc. Natl. Acad. Sci. USA* **88**, 6916–6920.
11. Burley, S. K., David, P. R., Sweet, R. M., Taylor, A. & Lipscomb, W. N. (1992) *J. Mol. Biol.* **224**, 113–140.
12. Jurnak, F., Rich, A., van Loon-Klaassen, L., Bloemendal, H., Taylor, A. & Carpenter, F. H. (1977) *J. Mol. Biol.* **112**, 149–153.
13. Eichele, G., Ford, G. C. & Jansonius, J. N. (1979) *J. Mol. Biol.* **135**, 513–516.
14. Thaller, C., Weaver, L. H., Eichele, G., Wilson, E., Karlsson, R. & Jansonius, J. N. (1981) *J. Mol. Biol.* **147**, 465–469.
15. Teng, T.-Y. (1990) *J. Appl. Crystallogr.* **23**, 387–391.
16. Petsko, G. A. (1975) *J. Mol. Biol.* **96**, 381–392.
17. Blum, M., Metcalf, P., Harrison, S. C. & Wiley, D. C. (1987) *J. Appl. Crystallogr.* **20**, 235–242.
18. Brünger, A. T., Kuriyan, J. & Karplus, M. (1987) *Science* **235**, 458–460.
19. Brünger, A. T. (1992) X-PLOR Manual (Yale Univ., New Haven, CT), Version 3.0.
20. Jones, T. A. (1985) *Methods Enzymol.* **115**, 157–171.
21. Carrell, C. J., Carrell, H. L., Erlebacher, J. & Glusker, J. P. (1988) *J. Am. Chem. Soc.* **110**, 8651–8656.
22. Arnett, E. M. (1963) *Prog. Phys. Org. Chem.* **1**, 223–403.
23. Brown, H. C., McDaniel, D. H. & Häflinger, O. (1955) in *Determination of Organic Structures by Physical Methods*, eds. Braude, E. A. & Nachod, F. C. (Academic, New York), Vol. 1, pp. 567–662.
24. Cox, R. A. & Yates, K. (1978) *J. Am. Chem. Soc.* **100**, 3861–3867.
25. Cox, R. A., Druet, L. M., Klausner, A. E., Modro, T. A., Wan, P. & Yates, K. (1981) *Can. J. Chem.* **59**, 1568–1573.
26. Grant, H. M., McTigue, P. & Ward, D. G. (1983) *Aust. J. Chem.* **36**, 2211–2218.
27. Cotton, F. A. & Wilkinson, G. (1988) *Advanced Inorganic Chemistry* (Wiley/Interscience, New York), p. 343.
28. Smith, E. L. & Spackman, D. H. (1955) *J. Biol. Chem.* **212**, 271–299.
29. Stirling, C. J., Colloms, S. D., Collins, J. F., Szatmari, G. & Sherratt, D. J. (1989) *EMBO J.* **8**, 1623–1627.
30. Groves, J. T. & Olson, J. R. (1985) *Inorg. Chem.* **24**, 2715–2717.